

Article

New Isocoumarin and Pyrone Derivatives from the Chinese Mangrove Plant *Rhizophora mangle*-Associated Fungus *Phomopsis* sp. DHS-11

Zhikai Guo ^{1,*}, Biting Chen ^{1,2}, Dandan Chen ², Xiaoling Deng ², Jingzhe Yuan ¹, Shiqing Zhang ¹, Zijun Xiong ¹ and Jing Xu ^{2,*} 

- ¹ Hainan Key Laboratory of Tropical Microbe Resources, Institute of Tropical Bioscience and Biotechnology, Chinese Academy of Tropical Agricultural Sciences & Key Laboratory for Biology and Genetic Resources of Tropical Crops of Hainan Province, Hainan Institute for Tropical Agricultural Resources, Haikou 571101, China; cbt688228@163.com (B.C.); yuanjingzhe@itbb.org.cn (J.Y.); zhangshiqing@itbb.org.cn (S.Z.); xiongzijun@itbb.org.cn (Z.X.)
- ² School of Chemical Engineering and Technology, Hainan University, Haikou 570208, China; 17769570501@163.com (D.C.); 20081700210002@hainanu.edu.cn (X.D.)
- * Correspondence: guozhikai@itbb.org.cn (Z.G.); happyjing3@163.com (J.X.)

Abstract: Mangrove-associated fungi are important sources for the discovery of new bioactive natural products. Three new isocoumarins (**1–3**) and one new pyrone derivative (**4**) were isolated from the ethyl acetate extract of the fermentation broth of the mangrove endophytic fungus *Phomopsis* sp. DHS-11. Nuclear magnetic resonance (NMR) spectroscopy (one-dimensional and two-dimensional) and mass spectrometry were used to determine the structures of these new compounds. The absolute configurations for the new isocoumarins **1–3** were determined by comparing their experimental and calculated electronic circular dichroism (ECD) spectra, while the configuration for the new pyrone-derivative **4** was tentatively solved by comparison of its ¹³C NMR data with reported data. In the biological activity test, compounds **1** and **3** showed cytotoxic activity against HeLa cells with IC₅₀ values of 11.49 ± 1.64 μM and 8.70 ± 0.94 μM, respectively. The initial structure and activity relationship (SAR) analysis revealed that the length of the side chain at C-3 for isocoumarin-type compounds **1–3** could affect the cytotoxicity against HeLa cells. Compound **4** exhibited cytotoxic activities against human hepatoma cells HepG2 with an IC₅₀ value of 34.10 ± 2.92 μM. All compounds have no immunosuppressive activity.

Keywords: mangrove; endophytic fungus; *Phomopsis* sp.; polyketides; cytotoxic activity



Citation: Guo, Z.; Chen, B.; Chen, D.; Deng, X.; Yuan, J.; Zhang, S.; Xiong, Z.; Xu, J. New Isocoumarin and Pyrone Derivatives from the Chinese Mangrove Plant *Rhizophora mangle*-Associated Fungus *Phomopsis* sp. DHS-11. *Molecules* **2023**, *28*, 3756. <https://doi.org/10.3390/molecules28093756>

Academic Editors: Simona Fabroni, Krystian Marszałek and Aldo Todaro

Received: 6 April 2023
Revised: 21 April 2023
Accepted: 26 April 2023
Published: 27 April 2023



Copyright: © 2023 by the authors. Licensee MDPI, Basel, Switzerland. This article is an open access article distributed under the terms and conditions of the Creative Commons Attribution (CC BY) license (<https://creativecommons.org/licenses/by/4.0/>).

1. Introduction

Marine-derived fungi are important sources for the discovery of natural products with unique structures and significant pharmacological activities [1–4]. Mangrove plants grow in saline-alkali habitats at the junction of tropical and subtropical climates, land and ocean, and endophytic fungi inhabiting them are the second-largest ecological group among marine fungi [5–8]. Endophytes are a group of parasitic species living in the tissue of plants without causing any obvious pathogenic symptoms [9]. Mangrove endophytic fungi form prolific metabolic pathways and adaptive mechanisms in unique environments, which produces a large number of natural secondary metabolites with novel structures and biological significance, such as terpenes, polyketides, alkaloids, etc., attracting extensive attention in drug mining and agrochemical applications [10–13]. *Phomopsis* sp. is a ubiquitous fungus and research on the secondary metabolites of this genus from a chemical point of view has shown that a variety of biologically active products have been found [14,15], such as lung cancer prevention potential drug cytochalasin, antibacterial chromones, antifungal lactones, and cytotoxic sesquiterpenes, etc., [16–20].

Previously, our research group has found many bioactive secondary metabolites from mangrove-plant-derived endophytic fungi from the Dong Zhai Gang mangrove garden in Hainan [21–23]. Recently, the fungus *Phomopsis* sp. DHS-11 was isolated from the root of freshly harvested mangrove plant, *Rhizophora mangle*. Preliminary phytochemical investigation on the fermentation products of the mangrove endophyte *Phomopsis* sp. DHS-11 led to the discovery of norpestaphthalides and a cerebroside-type natural compound, alternaroside B; however, biological tests showed that none of them had cytotoxic or immunosuppressive activities [24]. As part of our ongoing exploration of new and bioactive natural product targets in endophytic fungi of Hainan mangrove plants, one new pyrone-type and three new isocoumarin-type polyketides were isolated from the fermentation broth of *Phomopsis* sp. DHS-11, including phomoisocoumarin E (1), phomodihydroisocoumarin A (2), phomoisocoumarin F (3), and phomopyrone D (4) (Figure 1). Herein, we report the isolation of these compounds, the elucidation of their structures, and their biological activities.

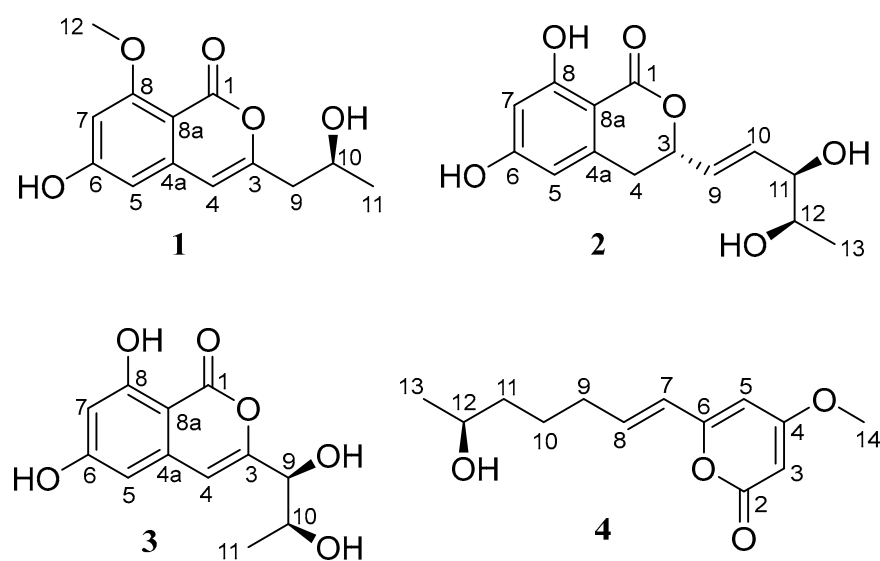


Figure 1. The chemical structures of compounds 1–4.

2. Results

2.1. Structure Elucidation of the New Compounds

Compound 1 was isolated as an amorphous powder. Its molecular formula of $C_{13}H_{14}O_5$ was determined by high-resolution electrospray ionization mass spectroscopy (HRESIMS) [m/z 249.0774 [$M - H$] $^-$ (calcd for $C_{13}H_{13}O_5$, 249.0768)], possessing seven degrees of unsaturation. According to the 1H NMR (Figure S1) data of compound 1 (Table 1), there were three aromatic proton signals at δ_H 6.25 (1H, s, H-4), 6.31 (1H, s, H-5), and 6.40 (1H, s, H-7). In addition, two methylene proton signals at δ_H 2.45 (1H, dd, $J = 14.2, 7.1$ Hz, H-9a) and 2.41 (1H, dd, $J = 14.2, 5.6$ Hz, H-9b), an oxygenated methine proton signal at 3.96 (1H, m, H-10), a methyl proton signal at δ_H 1.12 (3H, d, $J = 6.2$ Hz, H-11), a methoxyl proton signal at δ_H 3.80 (3H, s, H-12), and a hydroxyl group signal at δ_H 4.78 (1H, brs, OH-10) were present. The ^{13}C NMR (Figure S2) and DEPT135 (Figure S3) data (Table 2) showed that compound 1 contained thirteen carbons, including an ester carbonyl carbon, eight aromatic or olefinic carbons (three of which are protonated), a methylene carbon, an oxygenated methine carbon, and two methyl carbons. The data for compound 1 were similar to those of pestalotiorin, which were reported in the literature [25]. The major difference was the absence of a methyl group at C-7 in compound 1. The 1H - 1H COSY correlations from H-10 to H₂-9 and H₃-11 and key HMBC correlations from H-4 to C-5, C-4a, C-8a, C-3, and C-9, from H-7 to C-1, C-5, C-6, C-8, and C-8a, and from H₃-12 to C-8 were observed. Additionally, the methoxyl protons (H₃-12) only showed NOE correlation with H-7, permitting the location of the methoxyl group at C-8. The overall analysis of

the HSQC, HMBC, NOESY, and MS spectra (Figure 2 and Figures S4–S8) led to the full assignment of the structure as shown in Figure 1. We tried to use the modified Mosher's method to determine the absolute configuration of C-10 in compound **1** but without success. Thus, the absolute configuration of C-10 was tentatively determined to be 10S based on its specific rotation and calculated ECD spectrum (Figure 3). Therefore, the structure of compound **1** was identified and named phomoisocoumarin E.

Table 1. ¹H NMR (500 MHz) spectroscopic data of compounds **1–4**.

| Position | 1 ^a | 2 ^a | 3 ^a | 4 ^b |
|----------|---|--|---------------------------------------|---------------------------------------|
| | δ_{H} , Mult. (J in Hz) | δ_{H} , Mult. (J in Hz) | δ_{H} , Mult. (J in Hz) | δ_{H} , Mult. (J in Hz) |
| 3 | | 5.14, ddd (10.0, 5.6, 4.3) | | 5.47, d (2.1) |
| 4 | 6.25, s | 3.00, dd (12.7, 3.8); 2.92, dd (16.4, 10.1) | 6.59, s | |
| 5 | 6.31, s | 6.27, d (1.8) | 6.42, d (1.9) | 5.95, d (2.1) |
| 7 | 6.40, s | 6.20, d (1.8) | 6.33, d (1.9) | 6.04, d (15.6) |
| 8 | | | | 6.69, dt (15.6, 7.2) |
| 9 | 2.45, dd (14.2, 7.1); 2.41, dd (14.2, 5.6) | 5.78, dd (15.6, 6.5) | 3.98, d (6.5) | 2.17, m |
| 10 | 3.96, m | 5.98, dd (15.6, 5.0) | 3.80, qui (6.3) | 1.66–1.58, m; 1.57–1.48, m |
| 11 | 1.12, d (6.2) | 3.79, t (4.9) | 1.12, d (6.2) | 1.53–1.42, m |
| 12 | 3.80, s | 3.45, qui (6.0) | | 3.64, m |
| 13 | | 1.01, d (6.3) | | 1.06, d (6.2) |
| 14 | | | | 3.76, s |
| 8-OH | | 11.09, br s | 11.00, s | |
| 9-OH | | | 5.65, s | |
| 10-OH | 4.78, br s | | 4.78, s | |
| 11-OH | | 4.89, br s | | |
| 12-OH | | 4.52, br s | | |

^a Recorded in DMSO-*d*₆; ^b Recorded in CD₃OD.

Table 2. ¹³C NMR (125 MHz) spectroscopic data of compounds **1–4**.

| Position | 1 ^a | 2 ^a | 3 ^a | 4 ^b |
|----------|----------------------------|----------------------------|----------------------------|----------------------------|
| | δ_{C} , Type | δ_{C} , Type | δ_{C} , Type | δ_{C} , Type |
| 1 | 165.0, C | 169.1, C | 166.0, C | |
| 2 | | | | 167.0, C |
| 3 | 155.7, C | 78.4, CH | 157.6, C | 88.9, CH |
| 4 | 104.1, CH | 32.5, CH ₂ | 104.6, CH | 174.0, C |
| 4a | 141.7, C | 141.7, C | 139.3, C | |
| 5 | 102.8, CH | 107.1, CH | 103.2, CH | 101.1, CH |
| 6 | 158.0, C | 164.7, C | 162.6, C | 160.3, C |
| 7 | 98.9, CH | 100.9, CH | 101.7, CH | 122.8, CH |
| 8 | 163.1, C | 163.4, C | 165.4, C | 140.9, CH |
| 8a | 100.3, C | 100.1, C | 98.3, C | |
| 9 | 42.7, CH ₂ | 126.5, CH | 74.8, CH | 33.6, CH ₂ |
| 10 | 63.9, CH | 135.5, CH | 67.5, CH | 25.9, CH ₂ |
| 11 | 23.4, CH ₃ | 74.5, CH | 19.2, CH ₃ | 39.5, CH ₂ |
| 12 | 55.7, CH ₃ | 69.6, CH | | 68.3, CH |
| 13 | | 19.0, CH ₃ | | 23.5, CH ₃ |
| 14 | | | | 57.0, CH ₃ |

^a Recorded in DMSO-*d*₆; ^b Recorded in CD₃OD.

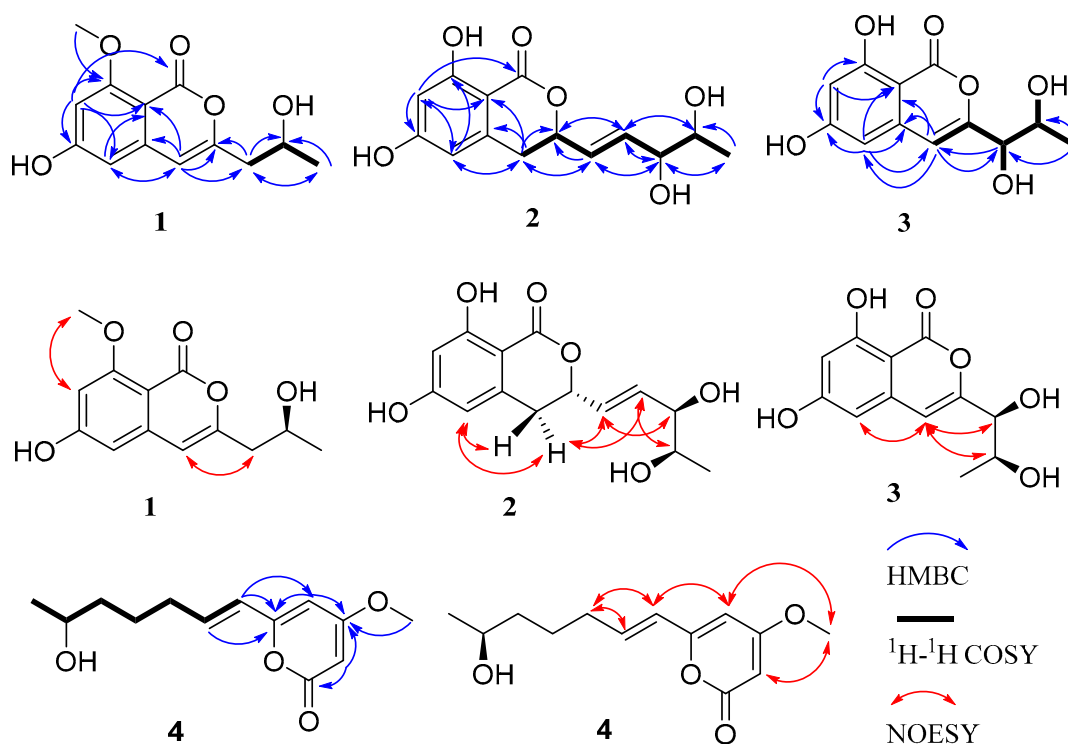


Figure 2. Key HMBC, ^1H - ^1H COSY, and NOESY NMR correlations of compounds 1–4.

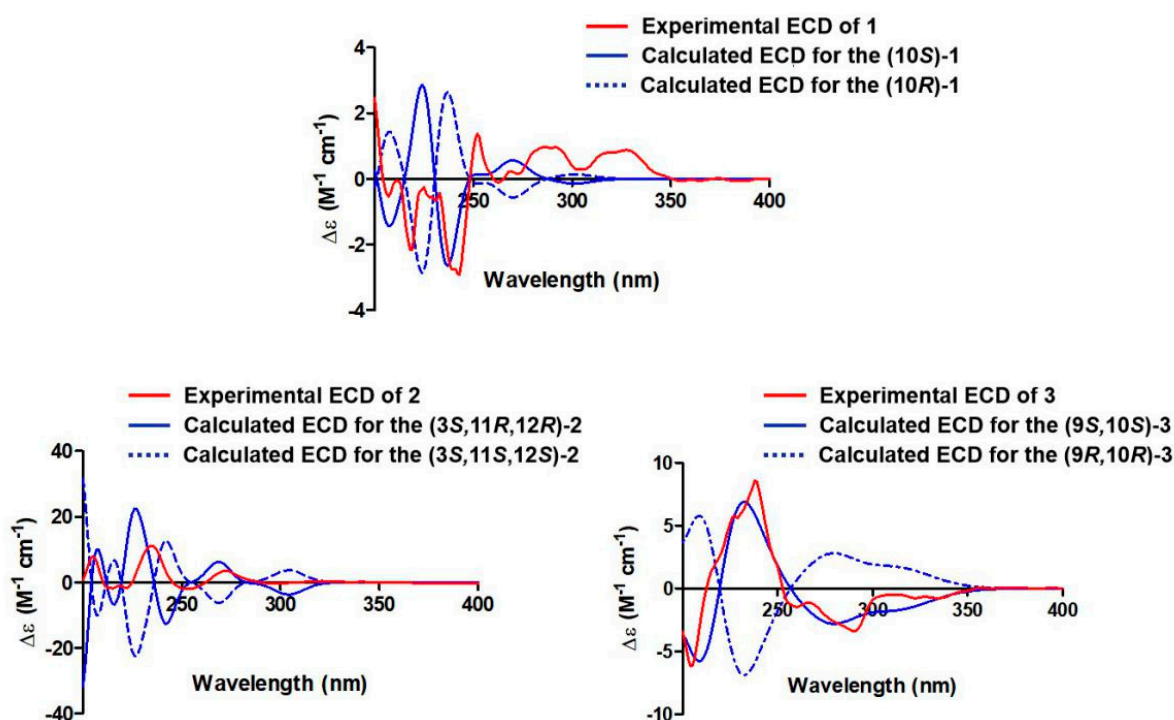


Figure 3. Comparison of experimental and calculated ECD spectra of compounds 1–3 in MeOH at the B3LYP/6-31+g (d, p) level.

Compound 2 was obtained as a white oil. HRESIMS data at m/z 281.1012 $[\text{M} + \text{H}]^+$ (calcd for $\text{C}_{14}\text{H}_{17}\text{O}_6$, 281.1020) (Figure S16) showed the molecular formula of $\text{C}_{14}\text{H}_{16}\text{O}_6$ with seven degrees of unsaturation. The IR absorption band at 3422 cm^{-1} suggested the presence of a hydroxyl group. The ^1H NMR data (Table 1 and Figure S9) indicated the presence of two meta-coupled aromatic proton signals at δ_{H} 6.20 (1H, d, $J = 1.8\text{ Hz}$, H-

7) and 6.27 (1H, d, $J = 1.8$ Hz, H-5), indicating the presence of a 1,2,3,5-tetrasubstituted aromatic ring. Analysis of the ^1H , ^{13}C (Table 2 and Figure S10), DEPT135 (Figure S11), and HSQC (Figure S12) NMR data revealed the presence of a methyl group, a methylene group, three oxygenated methine groups, eight aromatic or olefinic carbons (four of which are protonated), and an ester carbonyl group. Additionally, three hydroxyl proton signals at δ_{H} 11.09 (1H, s, 8-OH), 4.89 (1H, s, 11-OH or 12-OH), and 4.52 (1H, s, 11-OH or 12-OH) were observed. The ^1H - ^1H COSY (Figure 2 and Figure S14) spectrum showed correlations from H-12 to H₃-13 and H-11, from H-10 to H-9 and H-11, from H-9 to H-3 and H-10, and from H-3 to H-4 and H-9 (Figure 2). The HMBC spectra (Figure S13) correlations of H-9 with C-3 and C-4, H-7 with C-1, C-5, C-6, C-8, and C-8a, H-5 with C-4, C-7, and C-8a, and H₂-4 with C-3, C-4a, C-5, C-8a, and C-9 revealed an isocoumarin ring system (Figure 2). Comprehensive NMR analysis of HSQC, HMBC, NOESY, and MS data allowed the assignment of structure as shown in Figure 2. The *E* configuration of the olefinic bond C9-C10 was deduced by the large coupling constant ($J_{\text{H-9}/\text{H-10}} = 15.6$ Hz). The absolute configuration at C-3, C-11, and C-12 was determined to be 3*S*, 11*R*, and 12*R* by comparing the calculated ECD spectrum with the experimental ECD spectrum (Figure 3). Therefore, the structure of compound 2 was determined and named phomodihydroisocoumarin A.

Compound 3 was isolated as a viscous oil. It has a molecular formula of $\text{C}_{12}\text{H}_{12}\text{O}_6$ as determined by HRESIMS at m/z 275.0520 (calculated for $\text{C}_{12}\text{H}_{12}\text{NaO}_6$, 275.0526 $[\text{M} + \text{Na}]^+$) (Figure S24) and NMR spectrum (Figures S17–S23). Analysis of the ^1H NMR data (Table 1) revealed one methyl group signal at δ_{H} 1.12 (1H, d, $J = 6.2$ Hz, H₃-11), three aromatic proton signals at δ_{H} 6.59 (1H, s, H-4), 6.42 (1H, d, $J = 1.9$ Hz, H-5) and 6.33 (1H, d, $J = 1.9$ Hz, H-7), two oxygenated methine proton signals at δ_{H} 3.98 (1H, d, $J = 6.5$ Hz, H-9) and 3.80 (1H, qui, $J = 6.3$ Hz, H-10), and three hydroxyl proton signals at δ_{H} 11.00, 5.65, and 4.78. The ^{13}C NMR combined with DEPT135 spectra (Table 2) showed a total of 12 carbon signals, including one methyl group, two oxygenated methine groups, eight aromatic or olefinic carbons (three of which are protonated), and one ester carbonyl group. The ^1H and ^{13}C NMR data of 3 were very similar to those of compound 1. The distinction was attributed to the replacement of the methoxyl group at C-8 by a new phenolic hydroxyl group and the presence of a hydroxyl group at C-9 in 3. The HMBC, ^1H - ^1H COSY, and NOESY experiments (Figure 2) confirmed the deduction and allowed the assignment of structure as shown in Figure 1. Based on the analysis of the chemical shifts of C-9 (δ_{C} 74.8) and C-10 (δ_{C} 67.5) and the small coupling constant ($J_{\text{H-11}/\text{H-12}} = 6.5$ Hz), suggesting a *cis* configuration of C9 and C10 [26,27]. The relative configurations of C9 and C10 were also determined by NOESY correlations from H-4 to H-9 and H-10 (Figure 2). The absolute configurations of C9 and C10 were established as 9*S*,10*S* by comparison of their experimental ECD spectrum with the calculated ECD curves (Figure 3). Thus, compound 3 was identified as a new compound and named phomoisocoumarin F.

Compound 4 was obtained as an amorphous powder. Its molecular formula was deduced as $\text{C}_{13}\text{H}_{18}\text{O}_4$ by its HRESIMS data at m/z 261.1095 $[\text{M} + \text{Na}]^+$ (calcd for $\text{C}_{13}\text{H}_{18}\text{NaO}_4$, 261.1097) (Figure S32), indicating five degrees of unsaturation. The ^1H NMR spectrum (Figure S25) displayed one methyl proton signal at δ_{H} 1.06 (3H, d, $J = 6.2$ Hz, H-13), one methoxyl proton signal at δ_{H} 3.76 (3H, s, H-14), one oxygenated aliphatic methine proton signal at δ_{H} 3.64 (1H, m, H-12), four olefinic proton signals at δ_{H} 6.69 (1H, dt, $J = 15.6, 7.2$ Hz, H-8), 6.04 (1H, d, $J = 15.6$ Hz, H-7), 5.95 (1H, d, $J = 2.1$ Hz, H-5), 5.47 (1H, d, $J = 2.1$ Hz, H-3), and three sp^3 methylene proton signals at δ_{H} 2.17 (2H, m, H-9), 1.66–1.48 (2H, m, H-10), 1.53–1.42 (2H, m, H-11) (Table 1). The ^{13}C NMR spectrum (Figure S26) showed the presence of one methyl carbon signal at δ_{C} 23.5 (C-13) and one methoxyl carbon signal at δ_{C} 57.0 (C-14) (Table 2). The ^1H - ^1H COSY spectrum (Figure S30) of 4 revealed a spin system of H-7/H-8/H₂-9/H₂-10/H₂-11/H-12/H₃-13 (Figure 2). The *E* configuration of H-7 and H-8 was deduced from the large coupling constant ($J_{\text{H-7}/\text{H-8}} = 15.6$ Hz). The typical ^{13}C NMR data at δ_{C} 174.0 (C-4), 167.0 (C-2), 160.3 (C-6), 101.1 (C-5), 88.9 (C-3), and 57.0 (C-14) suggested the presence of a 6-substituted 4-methoxyl-2*H*-pyran-2-one (2-pyrone) moiety in 4 [28]. In the HMBC spectrum, key correlations from H-8 to C-6, from H-7 to C-5

and C-6, from H-5 to C-4 and C-6, and from H-3 to C-2 and C-4 allowed the connection of C-7 with C-6 on the 2-pyrone moiety (Figure 2). The methoxyl group positioned at C-4 of 2-pyrone moiety was secured by the observation of key HMBC correlations of H₃-14 with C-4 and NOE correlations (Figure S31) of H₃-14 with H-3 and H-5. The modified Mosher's method was applied to determine the absolute configuration of C-12 in **4** but without success. The planar structure of **4** was very similar to scirpyrone D, possessing the same stereocenter with one hydroxyl group. Due to almost the same chemical shifts of the chiral carbons (δ_C 68.3 for C-12 in **4** and δ_C 68.1 for C-4' in scirpyrone D) and opposite optical rotation values [-11.0 (c 0.10, MeOH) for **4** and 2.8 (c 0.60, MeOH) for scirpyrone D] [28], the absolute configuration of C-12 in **4** was determined to be 12S. Thus, the structure of **4** was elucidated as shown in Figure 1 and named phomopyrone D.

2.2. Biological Evaluation

The immunosuppressive and cytotoxic activities of compounds **1–4** were screened. For the cytotoxic activity test, all of these compounds (**1–4**) were first evaluated at the concentrations of 10 $\mu\text{g}/\text{mL}$. The result showed that only compounds **1**, **3**, and **4** had activity at this concentration. So the cytotoxic activities of these three compounds (**1**, **3**, and **4**) were evaluated in depth. The experimental results indicated that compounds **1** and **3** showed moderate inhibitory activities against human cervical cancer cells HeLa with IC₅₀ values of 11.49 ± 1.64 μM and 8.70 ± 0.94 μM , respectively, which is less active than the positive drug doxorubicin with IC₅₀ values of 0.95 ± 0.61 μM . The initial SAR analysis revealed that the length of the side chain at C-3 for isocoumarin-type compounds **1–3** could affect their cytotoxicity against HeLa cells, while the methoxyl modification at C-8 on the isocoumarin ring and the hydroxylation at C-9 on the side chain did not affect the activity. Simultaneously, only the pyrone derivative **4** exhibited significant cytotoxic activities against human hepatoma cells HepG2 with an IC₅₀ value of 34.10 ± 2.92 μM , comparable with the positive drug 5-fluorouracil with an IC₅₀ value of 21.69 ± 9.11 μM (Table 3), while all isolated isocoumarins **1–3** did not show activity when tested at the concentration of 10 $\mu\text{g}/\text{mL}$. However, all compounds have no immunosuppressive activity at the concentration of 10 $\mu\text{g}/\text{mL}$.

Table 3. Cytotoxic activities of compounds **1**, **3**, and **4** (IC₅₀, μM).

| Compounds | HeLa | HepG2 |
|----------------|------------------|------------------|
| 1 | 11.49 ± 1.64 | – |
| 3 | 8.70 ± 0.94 | – |
| 4 | – | 34.10 ± 2.92 |
| Doxorubicin | 0.95 ± 0.61 | – |
| 5-Fluorouracil | – | 21.69 ± 9.11 |

“–” no activity at the concentration of 10 $\mu\text{g}/\text{mL}$; “-” no data.

3. Materials and Methods

3.1. General Experimental Procedures

One-dimensional (1D) NMR (500 MHz for ¹H NMR and 125 MHz for ¹³C NMR) and two-dimensional (2D) NMR (HSQC, HMBC, ¹H-¹H COSY, ROSEY, or NOSEY) were measured on the Bruker AV-500 spectrometers (Bruker, Germany). The chemical shifts of ¹H and ¹³C NMR data were given in δ (ppm) and referenced to the solvent signal (CD₃OD, δ_H 3.31 and δ_C 49.00; DMSO-*d*₆, δ_H 2.50 and δ_C 39.52). High-resolution electrospray ionization mass spectroscopy (HRESIMS) data were acquired on an Agilent 6210 time-of-flight LC-MS instrument (Agilent Technologies Inc., Palo Alto, CA, USA). Optical rotation values were measured by JASCO P-1020 digital polarimeter (JASCO, Tokyo, Japan). IR spectrum data were recorded on Nicolet 380 Infrared Spectrometer (Thermo Fisher, Waltham, MA, USA). The electronic circular dichroism (ECD) data were determined using JASCO J-715 Spectropolarimeter (Jasco, Tokyo, Japan). The semipreparative high-performance liquid chromatography (HPLC) was equipped with an ODS column (250.0 mm \times 10.0 mm, 5

μm , Thermo Fisher Scientific, Waltham, MA, USA). Column chromatography (CC) was performed on silica gel (60–80 mesh or 200–300 mesh; Qingdao Marine Chemical Inc., Qingdao, China), Sephadex LH-20 (PharmaciaBiotec, Uppsala, Sweden), and ODS (40–70 μm , Nacalai Tesque, Kyoto, Japan).

3.2. Fungal Material and Culture Conditions

The endophytic fungus strain *Phomopsis* sp. DHS-11 was isolated from the living root of the mangrove plant *Rhizophora mangle* collected in Dong Zhai Gang mangrove garden on Hainan Island, China, in October 2015. It was identified as *Phomopsis* sp. by ITS gene sequence (GenBank Accession no. MT126606) analysis [29]. This strain was deposited and maintained in the research group of one of the authors, J.X. The strain *Phomopsis* sp. DHS-11 was cultivated on PDA medium (potato extract 200 g/L, glucose 20 g/L, agar 15 g/L, chloramphenicol 0.1 g/L) at 28 °C for 6 days. Then the agar blocks with mycelia were added into 130 × 1000 mL Erlenmeyer flasks containing 100 g rice and 100 mL of seawater (1000 mL conical flask with 100 mL seawater), then fermented for 35 days.

3.3. Extraction and Isolation

After fermentation, the whole fermentation mixtures of *Phomopsis* sp. DHS-11 were collected and mashed with a glass rod and extracted three times with ethyl acetate at room temperature. Then, the whole organic solvent was concentrated in vacuo to obtain 80 g of crude extract. The crude extract was fully mixed and ground with silica gel (60–80 mesh), then subjected to silica gel (200–300 mesh) CC eluted by gradient elution of $\text{CH}_2\text{Cl}_2/\text{MeOH}$ mixtures (*v/v*, 100:0, 100:1, 100:2, 100:4, 100:8, 100:16, 100:32, 100:64, 0:100) to obtain 9 fractions (Fr. 1–Fr. 9). The fraction Fr. 5 was eluted with gradient elution of $\text{CH}_2\text{Cl}_2/\text{MeOH}$ mixtures (*v/v*, 100:0–100:32) to obtain 5 subfractions (Fr. 5.1–Fr. 5.5). The subfraction Fr. 5.2 was applied to ODS CC with gradient elution of $\text{MeOH}/\text{H}_2\text{O}$ mixtures (*v/v*, 1:4, 3:7, 2:3, 1:1, 3:2, 7:3, 4:1, 0:1) and obtained five subfractions (Fr. 5.2.1–Fr. 5.2.5). The subfraction Fr. 5.2.2 was conducted on HPLC ($\text{MeOH}/\text{H}_2\text{O}$, 80:20, *v/v*; 3 mL/min, UV λ_{max} 254 nm) to obtain compound 1 (6 mg). The subfraction Fr. 5.3 was subjected to ODS CC eluted with gradient elution of $\text{MeOH}/\text{H}_2\text{O}$ (*v/v*, 1:4, 3:7, 2:3, 1:1, 3:2, 7:3, 4:1, 0:1) to yield subfractions Fr. 5.3.1–Fr. 5.3.4. The subfractions Fr. 5.3.1 and Fr. 5.3.2 were, respectively, purified by HPLC ($\text{MeOH}/\text{H}_2\text{O}$, 70:30 and 60:40, *v/v*; 3 mL/min, UV λ_{max} 254 nm) to yield compound 2 (4 mg) and compound 3 (5 mg); The fraction Fr. 6 was separated by silica gel CC eluted with gradient elution of $\text{CH}_2\text{Cl}_2/\text{MeOH}$ mixtures (*v/v*, 100:0–100:16) to obtain three components (Fr. 6.1–Fr. 6.3). The subfraction Fr. 6.1 was subjected to ODS CC using gradient elution of $\text{MeOH}/\text{H}_2\text{O}$ (*v/v*, 1:4, 3:7, 2:3, 1:1, 3:2, 7:3, 4:1, 0:1) to give fractions. The subfraction Fr. 6.2 was subjected to ODS CC using gradient elution of $\text{MeOH}/\text{H}_2\text{O}$ to yield four subfractions (Fr. 6.2.1–Fr. 6.2.4). The subfraction Fr. 6.2.3 was purified by Sephadex LH-20 CC to yield two subfractions (Fr. 6.2.3.1 and Fr. 6.2.3.2). The subfraction Fr. 6.2.3.2 was further separated by semi-preparative HPLC ($\text{MeOH}/\text{H}_2\text{O}$, 35:65, *v/v*; 3 mL/min, UV λ_{max} 254 nm) to afford compound 4 (2 mg).

Compound 1: amorphous powder, $[\alpha]_{\text{D}}^{25} + 3.000$ (*c* 0.10, MeOH); CD (*c* 0.05, MeOH) λ_{max} ($\Delta\epsilon$): 209 (−0.10), 211 (+0.04), 218 (−0.42), 237 (−0.49), 239 (−0.36), 243 (+0.34), 252 (+0.23) nm; IR (KBr) ν_{max} : 3424, 2923, 1700, 1654, 1600, 1441, 1373, 1160 cm^{-1} ; ^1H and ^{13}C NMR data, see Tables 1 and 2; HRESIMS *m/z* 249.0774 [$\text{M} - \text{H}$] $^-$ (calcd for $\text{C}_{13}\text{H}_{13}\text{O}_5$ 249.0768).

Compound 2: white oil, $[\alpha]_{\text{D}}^{25} + 7.000$ (*c* 0.10, MeOH); CD (*c* 0.05, MeOH) λ_{max} ($\Delta\epsilon$): 206 (+1.35), 234 (+1.92), 255 (−0.34), 272 (+0.60), 300 (−0.05) nm; IR (KBr) ν_{max} : 3422, 2925, 1630, 1517, 1466, 1381, 1167 cm^{-1} ; ^1H and ^{13}C NMR data, see Tables 1 and 2; HRESIMS *m/z* 281.1012 [$\text{M} + \text{H}$] $^+$ (calcd for $\text{C}_{14}\text{H}_{17}\text{O}_6$, 281.1020).

Compound 3: viscous oil, $[\alpha]_{\text{D}}^{25} - 20.000$ (*c* 0.10, MeOH); CD (*c* 0.05, MeOH) λ_{max} ($\Delta\epsilon$): 209 (−2.98), 237 (+6.50), 322 (−0.56) nm; IR (KBr) ν_{max} : 3422, 2923, 1681, 1628, 1460, 1382, 1238, 1170 cm^{-1} ; ^1H and ^{13}C NMR data, see Tables 1 and 2; HRESIMS *m/z* 275.0520 [$\text{M} + \text{Na}$] $^+$ (calcd for $\text{C}_{12}\text{H}_{12}\text{NaO}_6$, 275.0526).

Compound 4: amorphous powder, $[\alpha]_D^{25} - 11.000$ (c 0.10, MeOH); CD (c 0.05, MeOH) λ_{\max} ($\Delta\epsilon$): 205 (−0.16), 211 (−0.75), 218 (+0.11), 226 (−1.37) nm; IR (KBr) ν_{\max} : 3450, 2923, 1689, 1653, 1616, 1454, 1410, 1159 cm^{-1} ; ^1H and ^{13}C NMR data, see Tables 1 and 2; HRESIMS m/z 261.1095 $[\text{M} + \text{Na}]^+$ (calcd for $\text{C}_{13}\text{H}_{18}\text{NaO}_4$, 261.1097).

3.4. Electronic Circular Dichroism (ECD) Calculation Details

Monte Carlo conformational searches were conducted by means of Spartan's 14 software using Merck Molecular Force Field (MMFF). The conformers with Boltzmann-population of over 5% were chosen for ECD calculations, and then the conformers were initially optimized at B3LYP/6-31g level in gas. The theoretical calculations of ECD were carried out in MeOH using time-dependent density functional theory (TD-DFT) at the B3LYP/6-31+g (d, p) level for all conformers of compounds 1–3. Rotatory strengths for a total of 30 excited states were calculated. ECD spectra were generated using the program SpecDis 1.6 (University of Würzburg, Würzburg, Germany) and GraphPad Prism 5 (University of California San Diego, San Diego, CA, USA) from dipole-length rotational strengths by applying Gaussian band shapes with $\sigma = 0.3$ eV.

3.5. Cell Viability Assay

The antitumor activity of all isolated compounds 1–4 was evaluated as previously reported by using the MTT assay method [30]. At first, the antitumor activity of all of these isolated compounds (1–4) was evaluated at the concentrations of 10 $\mu\text{g}/\text{mL}$. Doxorubicin and 5-fluorouracil were used as positive control for human cervical cancer cells HeLa and human hepatoma cells HepG2, respectively. The prepared concentrations for each of compounds 1, 3, 4, and positive drugs in tests were 10, 5, 2.5, 1, 0.5, 0.1, 0.05, and 0.01 $\mu\text{g}/\text{mL}$, while compound 2 was only evaluated at the concentration of 10 $\mu\text{g}/\text{mL}$ as it displayed no activity. All cell lines were obtained from the Shanghai Cell Bank of the Chinese Academy of Sciences. The IC_{50} values of these compounds and positive controls were calculated after 24 h for HeLa cells and 48 h for HepG2 cells.

3.6. Immunosuppressive Assay

The immunosuppressive activity testing of compounds 1–4 was conducted with the previously reported CCK-8 assay method [30]. In the test, we set up three parallel trials, using cyclosporin A as the positive control, experiments of concanavalin A (ConA)-induced T cells, and lipopolysaccharide (LPS)-induced B cells. The concentrations of compounds 1–4, and cyclosporin A, ConA, and LPS were 10, 5, and 10 $\mu\text{g}/\text{mL}$, respectively. All mice were donated by the Hainan Medical College.

4. Conclusions

To summarize, four previously undescribed polyketides, including three new isocoumarins (1–3) and one new pyrone derivative (4), were obtained from the mangrove-derived fungus *Phomopsis* sp. DHS-11. The structures of these isolated compounds were determined by analysis of HRESIMS, 1D- and 2D-NMR, and ECD data. The antitumor activity assay suggested that the new pyrone compound 4 exhibited cytotoxic activities against human hepatoma cells HepG2 with an IC_{50} value of 34.10 ± 2.92 μM , comparable with the positive drug 5-fluorouracil, indicating that this new compound has the potential to develop novel anti-hepatoma drugs and deserves further study. In addition, two new isocoumarin-type compounds 1 and 3 showed inhibitory activities against human cervical cancer cells HeLa with IC_{50} values of 11.49 ± 1.64 μM and 8.70 ± 0.94 μM , respectively. In general, the results of this study expand the diversity of chemical constituents and biological activities isolated from the secondary metabolites of *Phomopsis* sp. DHS-11, and may provide new potential molecules for antitumor drug discovery. These results also prove that mangrove-associated fungi are still pools for mining new bioactive natural molecules.

Supplementary Materials: The following supporting information can be downloaded at: <https://www.mdpi.com/article/10.3390/molecules28093756/s1>, Figures S1–S32: 1D-, 2D-NMR, and MS spectra of compounds 1–4.

Author Contributions: Conceptualization, Z.G. and J.X.; methodology, Z.G. and B.C.; software, B.C. and J.Y.; validation, B.C. and J.Y.; formal analysis, Z.G. and J.X.; investigation, B.C., D.C. and X.D.; resources, Z.G.; data curation, B.C. and Z.G.; writing—original draft preparation, B.C. and Z.G.; writing—review and editing, Z.G. and J. X.; visualization, J.Y., S.Z. and Z.X.; supervision, Z.G. and J.X.; project administration, S.Z. and Z.X.; funding acquisition, Z.G. and J.X. All authors have read and agreed to the published version of the manuscript.

Funding: This research was financially supported by the Key Research Program of Hainan Province (ZDYF2023SHFZ107, ZDYF2021SHFZ108), the National Natural Science Foundation of China (82160675, 81973229), the Key Science and Technology Project of Hainan Province (ZDKJ202008, ZDKJ202018), and the Central Public-interest Scientific Institution Basal Research Fund for CATAS-ITBB (1630052022016, 1630052019011, 1630052023007).

Institutional Review Board Statement: Not applicable.

Informed Consent Statement: Not applicable.

Data Availability Statement: The authors declare that all relevant data supporting the results of this study are available within the article and its Supplementary Materials file, or from the corresponding authors upon request.

Conflicts of Interest: The authors declare no conflict of interest.

Sample Availability: Samples of compounds 1–4 are available from the authors.

References

1. Xu, J.; Yi, M.; Ding, L.; He, S. A review of anti-inflammatory compounds from marine fungi, 2000–2018. *Mar. Drugs* **2019**, *17*, 636. [[CrossRef](#)]
2. Zhu, X.C.; Huang, G.L.; Mei, R.Q.; Wang, B.; Sun, X.P.; Luo, Y.P.; Xu, J.; Zheng, C.J. One new α , β -unsaturated 7-ketone sterol from the mangrove-derived fungus *Phomopsis* sp. MGF222. *Nat. Prod. Res.* **2021**, *35*, 3970–3976. [[CrossRef](#)] [[PubMed](#)]
3. Zheng, C.J.; Shao, C.L.; Wu, L.Y.; Chen, M.; Wang, K.L.; Zhao, D.L.; Sun, X.P.; Chen, G.Y.; Wang, C.Y. Bioactive phenylalanine derivatives and cytochalasins from the soft coral-derived fungus, *Aspergillus elegans*. *Mar. Drugs* **2013**, *11*, 2054–2068. [[CrossRef](#)] [[PubMed](#)]
4. Guo, Z.; Gai, C.; Cai, C.; Chen, L.; Liu, S.; Zeng, Y.; Yuan, J.; Mei, W.; Dai, H. Metabolites with insecticidal activity from *Aspergillus fumigatus* JRJ111048 isolated from mangrove plant *Acrostichum speciosum* endemic to Hainan Island. *Mar. Drugs* **2017**, *15*, 381. [[CrossRef](#)]
5. Guo, Z.K.; Zhou, Y.Q.; Han, H.; Wang, W.; Xiang, L.; Deng, X.Z.; Ge, H.M.; Jiao, R.H. New antibacterial phenone derivatives asperphenone A–C from mangrove-derived fungus *Aspergillus* sp. YHZ-1. *Mar. Drugs* **2018**, *16*, 45. [[CrossRef](#)]
6. Deshmukh, S.K.; Agrawal, S.; Prakash, V.; Gupta, M.K.; Reddy, M.S. Anti-infectives from mangrove endophytic fungi. *S. Afr. J. Bot.* **2020**, *134*, 237–263. [[CrossRef](#)]
7. Chen, S.; Cai, R.; Liu, Z.; Cui, H.; She, Z. Secondary metabolites from mangrove-associated fungi: Source, chemistry and bioactivities. *Nat. Prod. Rep.* **2022**, *39*, 560–595. [[CrossRef](#)]
8. Chen, Y.; Zou, G.; Yang, W.; Zhao, Y.; Tan, Q.; Chen, L.; Wang, J.; Ma, C.; Kang, W.; She, Z. Metabolites with anti-inflammatory activity from the mangrove endophytic fungus *Diaporthe* sp. QYM12. *Mar. Drugs* **2021**, *19*, 56. [[CrossRef](#)]
9. Debbab, A.; Aly, A.H.; Proksch, P. Mangrove derived fungal endophytes—a chemical and biological perception. *Fungal Divers.* **2013**, *61*, 1–27. [[CrossRef](#)]
10. Dai, L.T.; Yang, L.; Kong, F.D.; Ma, Q.Y.; Xie, Q.Y.; Dai, H.F.; Yu, Z.F.; Zhao, Y.X. Cytotoxic indole-diterpenoids from the marine-derived fungus *Penicillium* sp. KFD28. *Mar. Drugs* **2021**, *19*, 613. [[CrossRef](#)]
11. Xu, J. Bioactive natural products derived from mangrove-associated microbes. *RSC Adv.* **2015**, *5*, 841–892. [[CrossRef](#)]
12. Carroll, A.R.; Copp, B.R.; Davis, R.A.; Keyzers, R.A.; Prinsep, M.R. Marine natural products. *Nat. Prod. Rep.* **2020**, *37*, 175–223. [[CrossRef](#)] [[PubMed](#)]
13. Xu, Z.; Xiong, B.; Xu, J. Chemical investigation of secondary metabolites produced by mangrove endophytic fungus *Phyllosticta capitalensis*. *Nat. Prod. Res.* **2021**, *35*, 1561–1565. [[CrossRef](#)] [[PubMed](#)]
14. Wei, C.; Sun, C.; Feng, Z.; Zhang, X.; Xu, J. Four new chromones from the endophytic fungus *Phomopsis asparagi* DHS-48 isolated from the Chinese mangrove plant *Rhizophora mangle*. *Mar. Drugs* **2021**, *19*, 348. [[CrossRef](#)]
15. Liu, Z.; Qiu, P.; Li, J.; Chen, G.; Chen, Y.; Liu, H.; She, Z. Anti-inflammatory polyketides from the mangrove-derived fungus *Ascomycota* sp. SK2YWS-L. *Tetrahedron* **2018**, *74*, 746–751. [[CrossRef](#)]

16. Dai, J.; Krohn, K.; Gehle, D.; Kock, I.; Flörke, U.; Aust, H.J.; Draeger, S.; Schulz, B.; Rheinheimer, J. New oblongolides isolated from the endophytic fungus *Phomopsis* sp. from *Melilotus dentata* from the shores of the Baltic Sea. *Eur. J. Org. Chem.* **2005**, *2005*, 4009–4016. [[CrossRef](#)]
17. Ma, Y.; Wu, X.; Xiu, Z.; Liu, X.; Huang, B.; Hu, L.; Liu, J.; Zhou, Z.; Tang, X. Cytochalasin H isolated from mangrove-derived endophytic fungus induces apoptosis and inhibits migration in lung cancer cells. *Oncol. Rep.* **2018**, *39*, 2899–2905. [[CrossRef](#)]
18. Ahmed, I.; Hussain, H.; Schulz, B.; Draeger, S.; Padula, D.; Pescitelli, G.; Van Ree, T.; Krohn, K. Three new antimicrobial metabolites from the endophytic fungus *Phomopsis* sp. *Eur. J. Org. Chem.* **2011**, *2011*, 2867–2873. [[CrossRef](#)]
19. Wu, S.H.; Chen, Y.W.; Shao, S.C.; Wang, L.D.; Li, Z.Y.; Yang, L.Y.; Li, S.L.; Huang, R. Ten-membered lactones from *Phomopsis* sp., an endophytic fungus of *Azadirachta indica*. *J. Nat. Prod.* **2008**, *71*, 731–734. [[CrossRef](#)]
20. Hentasin, C.; Kanokmedhakul, S.; Kanokmedhakul, K.; Hahnvajjanawong, C.; Soyong, K.; Prabpai, S.; Kongsaree, P. Cytotoxic pentacyclic and tetracyclic aromatic sesquiterpenes from *Phomopsis archeri*. *J. Nat. Prod.* **2011**, *74*, 609–613. [[CrossRef](#)]
21. Xu, Z.; Wu, X.; Li, G.; Feng, Z.; Xu, J. Pestalotiopsis B, a new isocoumarin derivative from the mangrove endophytic fungus *Pestalotiopsis* sp. HHL101. *Nat. Prod. Res.* **2020**, *34*, 1002–1007. [[CrossRef](#)] [[PubMed](#)]
22. Zhou, J.; Li, G.; Deng, Q.; Zheng, D.; Yang, X.; Xu, J. Cytotoxic constituents from the mangrove endophytic *Pestalotiopsis* sp. induce G0/G1 cell cycle arrest and apoptosis in human cancer cells. *Nat. Prod. Res.* **2018**, *32*, 2968–2972. [[CrossRef](#)] [[PubMed](#)]
23. Wei, C.; Deng, Q.; Sun, M.; Xu, J. Cytospyrone and cytosporarin: Two new polyketides isolated from mangrove endophytic fungus, *Cytospora* sp. *Molecules* **2020**, *25*, 4224. [[CrossRef](#)] [[PubMed](#)]
24. Chen, B.T.; Wu, W.C.; Zhou, D.D.; Deng, X.L.; Zhang, S.Q.; Yuan, J.Z.; Xu, J.; Guo, Z.K. Bioactive components of endophytic fungi from two Hainan mangrove plants. *J. Shenzhen Univ. Sci. Eng.* **2022**, *39*, 245–252. [[CrossRef](#)]
25. Arunpanichlert, J.; Rukachaisirikul, V.; Phongpaichit, S.; Supaphon, O.; Sakayaroj, J. Meroterpenoid, isocoumarin, and phenol derivatives from the seagrass-derived fungus *Pestalotiopsis* sp. PSU-ES194. *Tetrahedron* **2015**, *71*, 882–888. [[CrossRef](#)]
26. Lei, H.; Lin, X.; Han, L.; Ma, J.; Dong, K.; Wang, X.; Zhong, J.; Mu, Y.; Liu, Y.; Huang, X. Polyketide derivatives from a marine-sponge-associated fungus *Pestalotiopsis heterocornis*. *Phytochemistry* **2017**, *142*, 51–59. [[CrossRef](#)]
27. Chen, Y.; Liu, Z.; Liu, H.; Pan, Y.; Li, J.; Liu, L.; She, Z. Dichloroisocoumarins with potential anti-inflammatory activity from the mangrove endophytic fungus *Ascomycota* sp. CYSK-4. *Mar. Drugs* **2018**, *16*, 54. [[CrossRef](#)]
28. Tian, J.-F.; Yu, R.-J.; Li, X.-X.; Gao, H.; Guo, L.-D.; Tang, J.-S.; Yao, X.-S. ¹H and ¹³C NMR spectral assignments of 2-pyrone derivatives from an endophytic fungus of *sarcosomataceae*. *Magn. Reson. Chem.* **2015**, *53*, 866–871. [[CrossRef](#)]
29. Zhou, J.; Diao, X.; Wang, T.; Chen, G.; Lin, Q.; Yang, X.; Xu, J. Phylogenetic diversity and antioxidant activities of culturable fungal endophytes associated with the mangrove species *Rhizophora stylosa* and *R. mucronata* in the South China Sea. *PLoS ONE* **2018**, *13*, e019735. [[CrossRef](#)]
30. Xu, Z.Y.; Zhang, X.X.; Ma, J.K.; Yang, Y.; Zhou, J.; Xu, J. Secondary metabolites produced by mangrove endophytic fungus *Aspergillus fumigatus* HQD24 with immunosuppressive activity. *Biochem. Syst. Ecol.* **2020**, *93*, 104166. [[CrossRef](#)]

Disclaimer/Publisher’s Note: The statements, opinions and data contained in all publications are solely those of the individual author(s) and contributor(s) and not of MDPI and/or the editor(s). MDPI and/or the editor(s) disclaim responsibility for any injury to people or property resulting from any ideas, methods, instructions or products referred to in the content.